Fitoterapia 140 (2020) 104447

Contents lists available at ScienceDirect

Fitoterapia

journal homepage: www.elsevier.com/locate/fitote

Studies of blood–brain barrier permeability of gastrodigenin *in vitro* and *in vivo*

Yahui Mi[a,1], Yukang Mao[a,b,1], Huan Cheng[a], Guohan Ke[a], Mingping Liu[a,*], Chunping Fang[a], Qian Wang[a]

[a] School of Pharmacy, Guangzhou University of Chinese Medicine, Guangzhou, China
[b] Guangdong Shunde Innovative Design Institute, Foshan, China

ARTICLE INFO

Keywords:
Gastrodia elata
Gastrodigenin
Blood–brain barrier
hCMEC/D3
Microdialysis

ABSTRACT

According to the basic theories of traditional Chinese medicine, *Gastrodia elata* (*GE*) is clinically utilized for the treatment of cephalalgia and migraine. The gastrodigenin (*p*–hydroxybenzyl alcohol, HBA), one of the effective components of *GE*, may pass through the blood–brain barrier (BBB) to exert its pharmacological effects. This study aimed to investigate BBB permeability of HBA *via in vitro* hCMEC/D3 BBB model and *in vivo* microdialysis in rats. For the establishment of *in vitro* BBB model, hCMEC/D3 cells were used to construct the monolayer. The integrity of the monolayer was evaluated by TEER measurements, expression analysis of tight junction proteins (claudin-5, zo-1 and occludin) and apparent permeability coefficients (P_{app}) of fluorescein disodium. During the 6-day incubation of hCMEC/D3 cells, the values of TEER gradually increased and maintained above 100 $\Omega \cdot cm^2$. Besides, the expression levels of claudin-5 and zo-1 in hCMEC/D3 cells increased over time, and tended to be stable, suggesting that integrity of the monolayer has been completely established. Moreover, the P_{app} of fluorescein disodium was 3.94×10^{-7} $cm \cdot s^{-1}$ after administration for 180 min, indicating that the monolayer retains the characteristics of BBB and can restrict the diffusion of hydrophilic small-molecule compounds. A sensitive HPLC method was established for HBA detection, and the transport rate of HBA was assessed by a transwell system. HBA crossed the hCMEC/D3 BBB model rapidly, but a plateau was observed when HBA concentrations were relatively similar between the two sides of transwell. Permeability assay revealed that 32.91% of HBA could penetrate the *in vitro* BBB model after 240 min of administration. *In vivo* BBB permeability was evaluated by determining the concentrations of HBA in blood and brain simultaneously. Following HBA administration, the samples of microdialysis were collected at 20, 40 and 60 min, and then every 30 min until the procedure ended. Pharmacokinetic parameters of HBA showed that HBA could pass through BBB and reach its maximum concentration at 40 min in blood and brain tissue. Furthermore, AUC_{0-t} and AUC_{0-inf} for the brain–to–blood distribution ratio of HBA were 0.1925 and 0.2083, respectively, indicating that approximately 20% of HBA in blood could pass through the BBB and subsequently transported into the brain. Both *in vitro* and *in vivo* experiments confirmed that HBA could penetrate the BBB. In summary, the findings of this study highlight that a promising amount of HBA in blood can pass through the BBB and exerts its pharmacological effects on central nervous system (CNS) diseases.

1. Introduction

In traditional Chinese medicine, *Gastrodia elata* (*GE*) has been clinically used for treating different central nervous system (CNS) diseases, such as migraine, trigeminal autonomic cephalalgias and headache attributed to cranial and cervical vascular disorder [1]. According to the Chinese Pharmacopoeia, gastrodigenin (*p*–hydroxybenzyl alcohol, HBA; Fig. 1) is recognized as one of the main compounds for quality control of *GE*. HBA exerts pharmacological effects on CNS diseases by blocking oxidative stress, preventing brain injury [2] and improving viability of neural progenitor cells to protect nervous system against ischemic injury [3]. Drug molecules should pass through the blood–brain barrier (BBB) to exhibit their pharmacological activities on CNS diseases. Therefore, the promising therapeutic effects of HBA against CNS diseases indicate that this drug may cross BBB and play an important role in treating CNS diseases. However, it remains necessary

* Corresponding author.
E-mail address: liumingping@gzucm.edu.cn (M. Liu).
[1] These authors contributed equally to this work.

https://doi.org/10.1016/j.fitote.2019.104447
Received 4 October 2019; Received in revised form 30 November 2019; Accepted 30 November 2019
Available online 02 December 2019

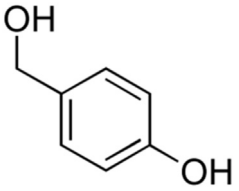

Fig. 1. Chemical structure of HBA.

to verify whether HBA can pass through BBB and the proportion of HBA transported into the brain.

The basic structure of BBB is relatively similar to brain microvascular endothelial cells and tight junction protein, which are indispensable for the establishment of *in vitro* BBB model. Tight junction between cells maintains the stability of brain microenvironment and blocks small-molecule drugs from BBB penetration. Specifically, claudin, occludin and zo are the major structural proteins of tight junction [4]. The hCMEC/D3 cell line, an immortalized cell line, has been proven to be reliable and feasible for BBB model establishment. This cell line exhibits similar morphological and functional characteristics as primary brain endothelial cells. A number of cell adhesion molecules in endothelial cells is also positively expressed in hCMEC/D3 cell line, and the positive expression of specific protein in endothelial cells can retain for at least 35 generations [5]. Moreover, ATP binding cassette (ABC) transporters, such as multidrug resistance proteins (MRP) and breast cancer resistance protein (BCRP), are highly expressed in hCMEC/D3 cell line [6]. In addition, hCMEC/D3 cell line retains morphological and functional characteristics of BBB even without co–culturing with glial cells [7].

For the *in vivo* assessment of BBB permeability, microdialysis can act as a useful and efficient technique because of its continuously and simultaneously drug monitoring in tissues and blood. Besides, it can also be used for the evaluation of brain pharmacokinetics apart from *in vivo* BBB penetration [8]. In addition to common pharmacokinetic parameters, brain–to–blood ratio is calculated to determine the amount of drug penetrating BBB, with simultaneous sampling from both blood and brain [9,10]. Although the pharmacokinetic parameters of HBA in blood have been reported [11], only a few studies have investigated the simultaneously sampling of blood and brain, brain–to–blood distribution of HBA, and *in vitro* BBB permeability of HBA.

The present study aimed to investigate the BBB permeability and pharmacokinetics of HBA through both *in vitro* and *in vivo* experiments. The integrity of hCMEC/D3 monolayer was established for *in vitro* BBB permeability assays. Simultaneous microdialysis of blood and brain in rats was used for the *in vivo* BBB penetration assessment of HBA.

2. Materials and methods

2.1. Chemicals and reagents

HBA was obtained from Sigma–Aldrich Co., Ltd. (St. Louis, USA). Fetal bovine serum (FBS) was purchased from Biological Industries Co., Ltd. (Kibbutz Beit Haemek, Israel). Roswell Park Memorial Institute 1640 (RPMI 1640), 0.25% Trypsin–EDTA and Hanks Balanced Salt Solution (HBSS) were purchased from Gibco Life Technologies (New York, USA). Antibodies of claudin-5, zo-1 and occludin were purchased from Santa Cruz Biotechnology, Inc. (Dallas, USA), while GAPDH antibody was obtained from Cell Signaling Technology, Inc. (Denver, USA). Transwell plates (polyethylene terephthalate membrane, pore size 0.4 μm) were purchased from Corning Costar (Cambridge, USA). The perfusates used for blood and brain microdialysis were Ringer's solution (RS; 147 mM NaCl, 4 mM KCl and 2.5 mM $CaCl_2$) and artificial cerebrospinal fluid solution (aCSF; 73 mM NaCl, 1.3 mM KCl, 0.6 mM $CaCl_2$ and 0.9 mM $MgCl_2$), which were purchased from Shanghai Hao Cai Biotechnology Co., Ltd. (Shanghai, China). The brain probe and blood probe were obtained from Shenzhen Ryward Life Technology Co., Ltd., Eicom (Shenzhen, China).

2.2. Cell lines and animals

The hCMEC/D3 cell line was supplied by JENNIO Biological Technology Co., Ltd. (Guangzhou, China). Adult male Sprague Dawley (SD) rats were purchased from the Laboratory Animal Center of Guangzhou University of Chinese Medicine. The animals, weighing between 180 and 220 g, were raised in a specifically pathogen–free environment. All animal experimentation was approved by the Animal Ethics Committee of Guangzhou University of Chinese Medicine (reg. SCXK Guangdong 2013–0020).

2.3. Instruments and HPLC methods

Transepithelial electrical resistance (TEER) was assessed by a Millipore Millicell ERS–2 V–ohm meter (Billerica, MA, USA), and the concentration of fluorescein disodium was determined by a Hitachi F–2500 fluorescence spectrophotometer (Tokyo, Japan).

HBA samples were analyzed on a Kromasil ODS column (250 mm × 4.6 mm, 5.0 μm) using a Shimadzu LC–20 AT HPLC system (Kyoto, Japan). The microdialysis system included a MD–1000 microinjection pump and a MD–2310 probe, which were purchased from BASi (West Lafayette, USA).

The mobile phase contained a mixture of methanol (A) and 0.5% phosphoric acid (B), and the gradient elution (A: 10% and B: 90%) was employed at a flow rate of 1 $ml{\cdot}min^{-1}$. The injection volume and detection wavelength were set at 10 μl and 220 nm, respectively.

2.4. Cell cultures

The complete medium was consisted of 90% RPMI 1640 and 10% FBS. The hCMEC/D3 cells were seeded at a density of 2×10^5 cells per well in transwell plates, and the bottom of the plates was maintained with the same medium at 37 °C in a humidified atmosphere containing 5% CO_2. The culture medium was changed and TEER was determined every two days. TEER of > 100 $\Omega{\cdot}cm^2$ was selected for the determination of HBA [[12]].

2.5. Western blotting

After incubation for 2, 4, 6, 8 and 10 days, hCMEC/D3 cells were lysed with RIPA buffer on ice for 15 min, followed by centrifugation at 13000 rpm for 10 min at 4 °C. Protein samples were separated by 10% SDS–PAGE, and then transferred onto polyvinylidene fluoride membrane (PVDF; Millipore, USA). Subsequently, the membrane was blocked with buffer containing 5% BSA, Tris (20 mM, pH 7.4), NaCl (75 mM) and Tween 20 (1%) at room temperature for 1 h. After that, the membrane was incubated with primary antibodies overnight at 4 °C, followed by secondary antibody at room temperature for 1 h. Finally, the membrane was incubated with electrochemiluminescence (ECL; Millipore, USA) substrate for 2 min, and Image J was used to analyze the grey values of the image. Grey value was calculated as the ratio of grey value of sample protein to grey value of GAPDH.

2.6. Fluorescein disodium permeability assay

Before starting the experiments, the barrier integrity of hCMEC/D3 cell monolayers was examined by TEER, and only the monolayer with TEER > 100 $\Omega{\cdot}cm^2$ was selected. Permeability assays were conducted by adding HBSS containing fluorescein disodium (100 $\mu g{\cdot}ml^{-1}$) to the apical side (AP) and injecting blank HBSS into the basolateral side (BL). After incubation for 180 min, 100 μl of medium was collected from the BL. Fluorescence intensities of the samples were measured, and P_{app} (AP → BL) was calculated as follows: $P_{app} = (\Delta C/\Delta t)/(C_0 A)$, where $\Delta C/$

Δt represents the change in FLU concentration over time, C_0 is 100 μg·ml^{-1}, and A is 4.67 cm^2.

2.7. Transport of HBA across hCMEC/D3 cell monolayer

Prior to the experiments, the cells were washed with warm HBSS. After TEER examination of hCMEC/D3 cell monolayers (> 100 Ω·cm^2), HBA dissolved in HBSS (200 μg·ml^{-1}) was added to the AP side, while blank HBSS was injected into the BL side. Aliquots (200 μl) of medium were collected from the BL at 10, 20, 40, 60, 90, 120, 180 and 240 min, and then replaced with the corresponding volume of HBSS. For HBA determination, the samples were injected into the HPLC system without preliminary treatment.

2.8. Validation of HBA determinative method

For calibration curve, seven concentrations of calibration standards were processed. The contents of HBA in samples were calculated by the obtained calibration curve within the same day. LLOQ (Lower Limit of Quantification) was defined at which an acceptable accuracy within ± 20% and precision below 20% can be obtained, by considering a signal–to–noise ratio of 10:1. The inter–day and intra–day precision assays were carried out at three levels, with five replicates for each of the three batches on three consecutive days.

2.9. Probe calibration

Probes of brain and blood were inserted into the right hippocampus and jugular vein, respectively. The relative recovery (RR%) and relative loss (RL%) at different flow rates, different drug concentrations and 8-h stability *in vivo* were calculated as follows: RR% = $C_{dialysis}$/$C_{perfusate}$ × 100%; RL% = ($C_{perfusate}$–$C_{dialysis}$)/$C_{perfusate}$ × 100%. RS and aCSF were used as the blank perfusates for vascular perfusion and cerebral perfusion, respectively.

For flow rate calibration, HBA was dissolved in blank perfusates (30.96 μg·ml^{-1} in RS and 51.48 μg·ml^{-1} in aCSF) and perfusion was conducted under different flow rates (1.0, 1.5, 2.0 and 2.5 μg·ml^{-1}). The concentrations of HBA in the dialysates were determined prior to RR% and RL% calculation. For drug concentration calibration, different concentrations of HBA were dissolved in blank perfusates (10.32–30.96 μg·ml^{-1} in RS and 5.72–51.48 μg·ml^{-1} in aCSF) and perfusion was conducted. The concentrations of HBA in the dialysates were determined prior to RR% and RL% calculation. For probe stability test, the perfusion of HBA (30.96 μg·ml^{-1} in RS and 28.60 μg·ml^{-1} in aCSF) was conducted for 8 consecutive hours, and the dialysate was collected every 60 min at 2 μl·min^{-1} flow rate. The concentrations of HBA in the dialysates were determined prior to RL% calculation.

2.10. Pharmacokinetic study

Before starting the experiments, probes were settled in heparin sodium and perfused for 30 min to prevent cruor during perfusion. All the rats were fasted for 12 h, but had free access to water. The microdialysis probes for brain and blood were implanted in the right hippocampus and jugular vein, respectively. Following a complete probe implantation, HBA (24 mg·kg^{-1}) was orally administrated, and dialysates were collected at 20, 40 and 60 min, and afterwards every 30 min until the end of the experiment. The flow rate was set as 2 μl·min^{-1} during the entire microdialysis procedure. For HBA determination, the samples were injected into the HPLC system without preliminary treatment. Pharmacokinetic parameters were determined by non–compartmental analysis using the PKSolver 2.0.

2.11. Statistic analysis

Statistical calculations were performed using SPSS software version 19.0. One–way analysis of variance (ANOVA) followed by Student–Newman–Keuls test was used for multigroup comparisons. P < .05 was regarded as statistical significance.

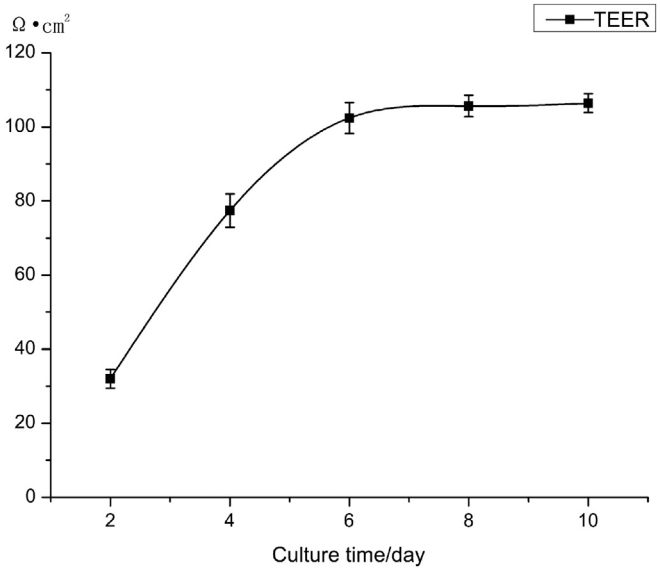

Fig. 2. Time–TEER curve of the integrity of hCMEC/D3 monolayer. (x ± s; n = 3).

3. Results

3.1. TEER curve

Time–TEER curve is shown in Fig. 2. TEER increased with culturing time until day 6, and then remained stable. The, stability of TEER indicated that hCMEC/D3 monolayer was completed on the basis of steady electrical resistance. Thus, the *in vitro* BBB model was established in this study.

The values of TEER inside and outside the Transwell inserts were measured every other day during BBB model establishment. The TEER values gradually increased and achieved > 100 Ω·cm^2 after day 6, implying the integrity of hCMEC/D3 cells is being enhanced [12]. During this state, the micropores on the polyester film were almost completely closed. These results indicated that the *in vitro* BBB model was well-established, and its barrier integrity was not damaged.

3.2. Expression of tight junction proteins

The expression levels of tight junction proteins are shown in Fig. 3. Fig. 3(A) demonstrates the expression levels of claudin-5, zo-1 and occludin. As illustrated in Fig. 3(B), the expression level of claudin-5 in hCMEC/D3 cells increased significantly until day 6, while that of zo-1 upregulated before day 4. These results indicated that the over-expression of claudin-5 and zo-1 in hCMEC/D3 cells retained their monolayer characteristics over time. However, the expression level of occludin in hCMEC/D3 cells did not change significantly throughout the incubation time.

The results of expression assays showed that tight junction proteins were obviously expressed in hCMEC/D3 cells, suggesting that hCMEC/D3 model could reflect the protein–related properties of *in vivo* BBB. Moreover, the expression levels of claudin-5 and zo-1 in hCMEC/D3 cells were significantly higher compared to the cells cultured for two and four days.

3.3. Permeability of fluorescein disodium

Fluorescein disodium can be used to detect the permeability of BBB,

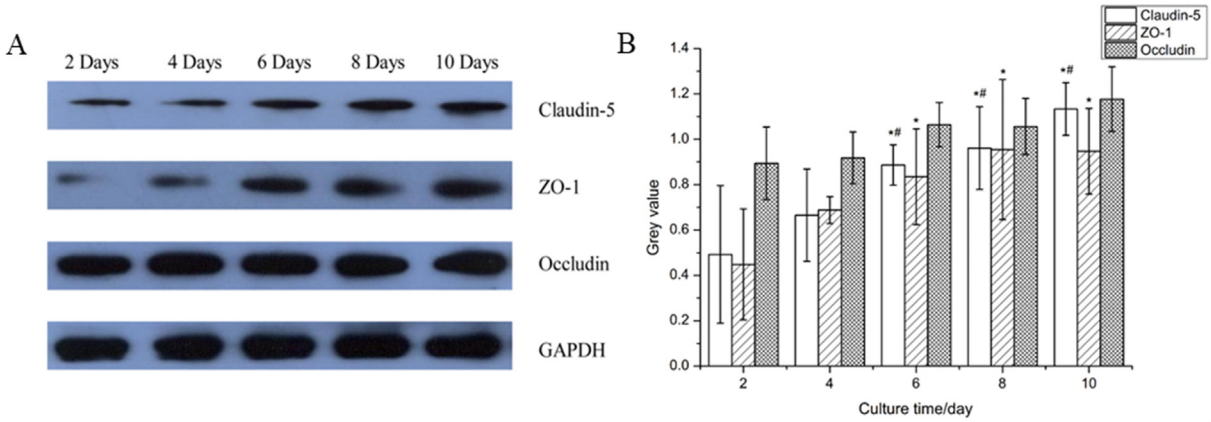

Fig. 3. Expression of the tight junction proteins in hCMEC/D3 cells. (A) The expression levels of claudin-5, zo-1 and occludin at different culture times *via* Western blot analysis. (B) Grey value analysis of protein blots. $^{*}P < .05$ *vs.* Day 2 group; $^{\#}P < .05$ *vs.* Day 4 group; x ± s; n = 3.

Table 1
Permeability of fluorescein disodium.

Time (min)	P_{app} (1×10^{-7} cm·s^{-1})
40	4.80 ± 0.40
80	4.27 ± 0.21
120	4.65 ± 0.08
180	3.94 ± 0.15

(x ± s; n = 3)

as this compound can hardly penetrate normal BBB. However, if BBB is damaged or with increased permeability, fluorescent signal can be clearly observed in brain tissue because fluorescein disodium is not restricted and pass through BBB. In this study, the P_{app} value of fluorescein disodium across BBB monolayer was evaluated, and the results are presented in Table 1.

After 180 min, the mean value of P_{app} in three duplicate samples was 3.94×10^{-7} cm·s^{-1}. BBB model established by hCMEC/D3 cells manifested restrictive permeability to small hydrophilic molecules, thus preventing the penetration of small hydrophilic molecules and maintaining cerebral homeostasis.

Fluorescein disodium is a hydrophilic small–molecule compound with no corresponding cell surface receptor, which is often restricted by BBB. Thus, the detection of fluorescein disodium permeability can be used to evaluate the restrictive capability of hydrophilic small–molecule substances. The P_{app} value of fluorescein disodium against *in vitro* BBB model established by hCMEC/D3 was $< 15 \times 10^{-6}$ cm·s^{-1}, implying that the permeability of fluorescein disodium is poor because drugs with $P_{app} < 15 \times 10^{-6}$ cm·s^{-1} are considered poor delivery across the BBB [13]. These results suggest that the established hCMEC/D3 model exhibits similar characteristics as *in vivo* BBB.

3.4. Establishment of HBA determinative method

Prior to BBB permeability measurement, a HPLC method was established to detect the concentrations of HBA. As demonstrated in Fig. 4, the residence time of HBA was 14.6 min. Typical linear regression equations for the calibration curves over HBA concentration ranges are shown in Table 2. HBA could be clearly differentiated and quantitatively determined at the LLOQ level.

The intra– and inter–day precision of HBA were evaluated in five duplicate samples, at three concentration levels. The results are presented in Table 3.

Tables 2 and 3 point out that the proposed HPLC method has reliable linearity and precision, which fell within the acceptance criteria of HBA determination.

3.5. Probe calibration

The results of probe calibration are shown in Tables 4-6. RR% and RL% fluctuated slightly over different concentrations of HBA in RS (10.32–30.96 μg·ml^{-1}) and aCSF (5.72–51.48 μg·ml^{-1}), indicating that the probe can remain stable during HBA perfusion. Moreover, according to the stability of probe implanted in both vessel and brain, the *in vivo* reliability of this probe could maintain for at least 8 h. These findings demonstrated that the probe might not be significantly affected by flow rate and drug concentration during microdialysis, and was stable for 8 h *in vivo*.

The reverse dialysis method has used to determine the relative loss rate of the probe to the drug, which is reliable for probe calibration [14]. In addition, this method is also simple, time–saving and convenient for the determination of HBA.

3.6. In vitro BBB permeability of HBA

As shown in Fig. 5, the concentrations of HBA were increased in hCMEC/D3 cells within 40 min. The transport rates of HBA across the BBB increased rapidly to 31.44% in 10 min, and then raised to 40.29%. Following that, the transport rates of HBA decreased gradually and retained at 32.91% after treatment for 4 h. This indicates that the permeability of BBB is promising when there was an obvious difference in HBA concentrations between the two sides of transwell, but a plateau could be observed when HBA concentrations were relatively similar between the two sides of transwell.

3.7. Pharmacokinetic study of HBA in blood and brain

After being anesthetized by an intraperitoneal injection of urethane, the head and skin of rats were shaved and disinfected with 70% ethanol, respectively, prior to the surgery. After exposing the skull with a 2-cm midline incision, a micro drill was used to implant the catheter through a 0.9-mm hole (AP + 0.2 mm, MR + 3.5 mm), and lowered to a depth of 3 mm ventral to the dura surface. The entire surgical process was completed within 30 min, and antidote was used to terminate the anesthesia. After three days, the animals were anesthetized with 25% urethane. The brain probe was inserted into the catheter carefully to perfuse the aCFS at a flow rate of 2 μl·min^{-1} for 1 h. The blood probe was carefully implanted (approximately 2.5–3.0 mm), and RS was perfused at a flow rate of 2 μl·min^{-1} for 1 h.

The validated HPLC method was applied to determine the concentrations of HBA in blood and brain tissue. As shown in Table 7 and Fig. 6A, the pharmacokinetic data revealed that the concentrations of HBA increased to C_{max} at 40 min in both blood and brain tissue. Notably, the C_{max} values were 38.03 μg·ml^{-1} in blood and 10.60 μg·ml^{-1}

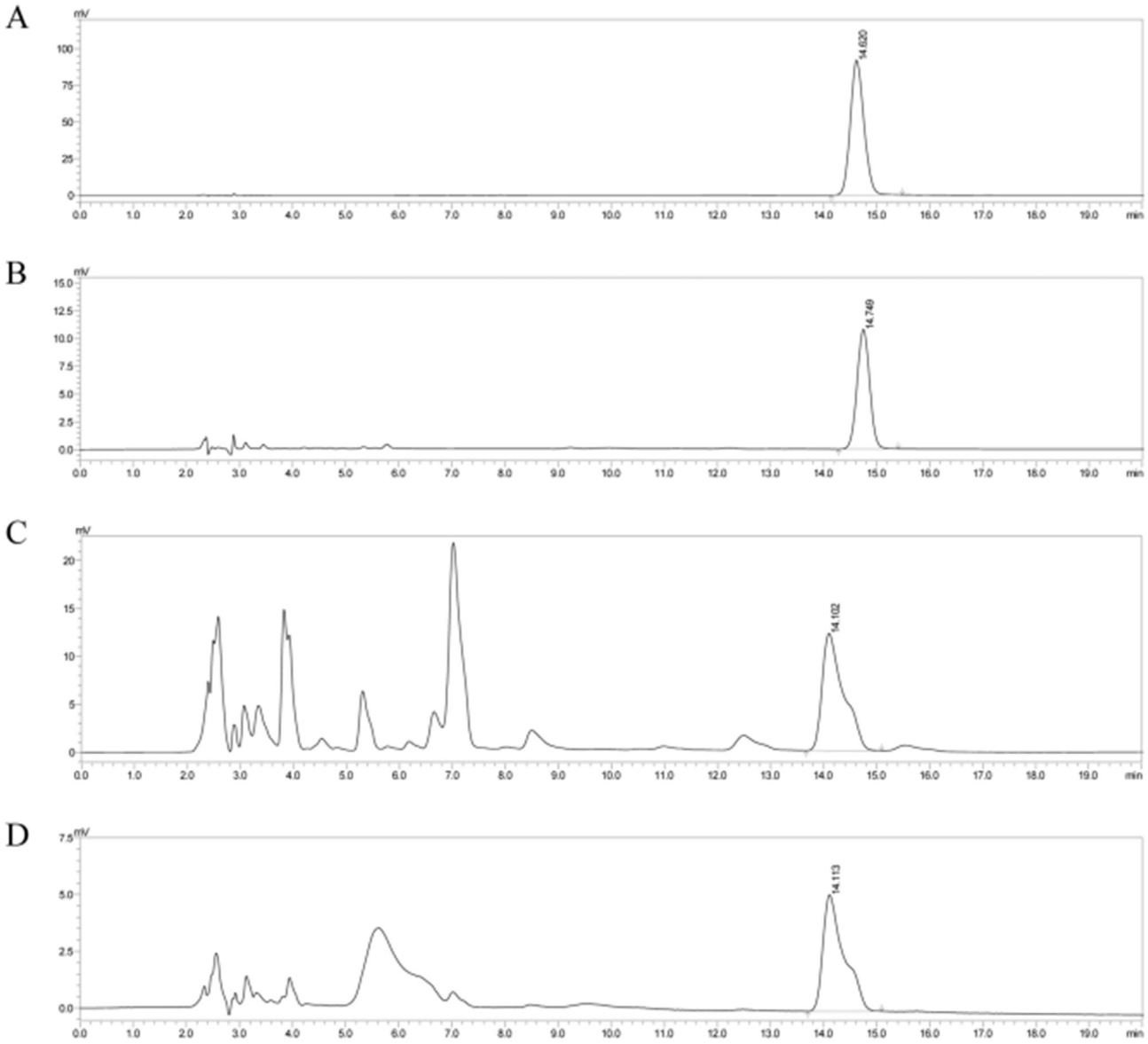

Fig. 4. HPLC chromatogram of HBA. (A) HBA standard solution; (B) sample of *in vitro* BBB permeability across hCMEC/D3 cells; (C) sample of blood microdialysis; and (D) sample of brain microdialysis.

Table 2
Regression equations, linear ranges and LLOQ of HBA.

Analyte	Linearity	R^2	Linear range ($\mu g \cdot ml^{-1}$)	LLOQ($\mu g \cdot ml^{-1}$)
In HBSS	Y = 36,238 X-77040	0.999	4.1–258.1	0.4
In RS	Y = 30,203 X-3711.3	1	0.4–51.6	0.4
In aCSF	Y = 45,886 X + 10,014	0.999	0.1–51.5	0.1

in brain after 40 min of administration, indicating that HBA can be absorbed into the bloodstream and transported across the BBB rapidly. However, $t_{1/2}$ demonstrated that half amount of HBA could be eliminated within 70.75 and 57.63 min in blood and brain, respectively. Moreover, the C_{max}, AUC_{0-t} and AUC_{0-inf} of HBA were higher in blood than in brain tissue. The values of AUC_{0-t} and AUC_{0-inf} were 5810.41 and 6076.32 $\mu g \cdot min \cdot ml^{-1}$ in blood, while 1115.32 and 1266.53 $\mu g \cdot min \cdot ml^{-1}$ in brain, respectively. Furthermore, AUC_{0-t} and AUC_{0-inf} for the brain–to–blood distribution ratio (AUC_{brain}/AUC_{blood}) of HBA were 0.1925 and 0.2083, suggesting that approximately 20% of HBA in blood penetrates the BBB and exerts pharmacological effects on CNS diseases.

Table 3
Intra– day and inter– day precision of HBA.

Analyte	Concentration ($\mu g \cdot ml^{-1}$)	Intra–day RSD%	Inter–day RSD%
In HBSS	129.38	1.17	0.07
	36.11	3.28	0.69
	9.14	2.93	3.37
In RS	30.96	1.19	1.95
	10.32	1.14	1.15
	0.42	4.88	8.22
In aCSF	34.32	0.11	0.75
	11.44	0.47	1.11
	0.14	0.93	3.13

4. Discussion

hCMEC/D3 cell line is considered as a reliable tool for the establishment of *in vitro* BBB model, as this cell line is screened from the

Table 4
Flow rate calibration of probes in blood and brain.

Probe	Flow rate (μl·min^{-1})	RR%	RL%
In blood	1.0	50.80 ± 0.11	48.06 ± 0.96
	1.5	47.04 ± 2.36	41.79 ± 0.33
	2.0	45.06 ± 0.02	40.11 ± 0.22
	2.5	37.64 ± 0.02	37.13 ± 0.16
In brain	1.0	50.76 ± 1.03	39.83 ± 0.51
	1.5	43.74 ± 1.27	42.84 ± 0.61
	2.0	41.64 ± 1.09	41.45 ± 0.30
	2.5	30.84 ± 0.83	43.42 ± 0.04

(x ± s; n = 4)

Table 5
HBA concentration calibration of probes in blood and brain.

Probe	Concentration (μl·min^{-1})	RR%	RL%
In blood	30.96	46.33 ± 0.39	42.17 ± 0.64
	20.64	45.46 ± 0.58	46.89 ± 0.11
	10.32	48.18 ± 1.15	49.09 ± 0.20
In brain	51.48	42.16 ± 0.54	39.83 ± 0.51
	28.60	38.33 ± 0.15	42.84 ± 0.61
	5.72	36.23 ± 0.04	43.42 ± 0.04

(x ± s; n = 4)

Table 6
Stability of HBA during microdialysis in blood and brain.

Probe	Mean of RL% in 8 h	SD of RL% in 8 h	RSD%
In blood	40.20	1.67	4.2
In brain	43.02	1.29	2.9

(x ± s; n = 4)

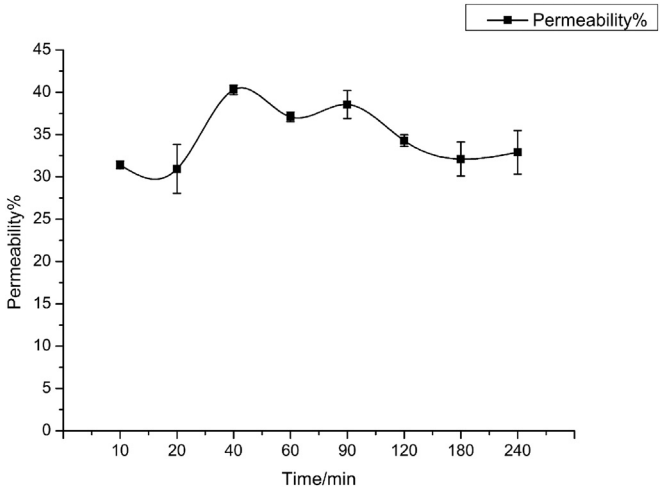

Fig. 5. Permeability of HBA through hCMEC/D3 BBB model. (x ± s; n = 4).

primary brain capillary endothelial cell lentivirus [15], and it displays similar characteristics as primary brain capillary endothelial cells, such as the comparable expression levels of tight junction proteins and chemokines. More importantly, *in vitro* BBB model can be established by hCMEC/D3 cells without the co–incubation of astrocytes [16]. Furthermore, the positive expression of signature proteins in hCMEC/D3 cells can maintain for at least 35 passages [4], which sustains the repeatability and reliability of the model. Therefore, hCMEC/D3 cell line was selected to establish an *in vitro* BBB model in the present study. In addition, the TEER value, tight junction protein expression and fluorescein disodium permeability of hCMEC/D3 cells were determined to evaluate their integrity and similarity to the *in vivo* BBB.

Table 7
Blood and brain microdialysis parameters for HBA.

Parameters	In blood	In brain
C_{max} (μg·ml^{-1})	38.03 ± 2.62	10.60 ± 1.55
T_{max}(min)	40	40
$T_{1/2}$ (min)	70.75 ± 5.98	57.63 ± 1.99
AUC_{0-t} (μg·min·ml^{-1})	5810.41 ± 603.85	1115.32 ± 71.58
AUC_{0-inf} (μg·min·ml^{-1})	6076.32 ± 600.57	1266.53 ± 131.68
CL/F(mg·kg^{-1})/(ml·μg^{-1})/h	0.239 ± 0.024	1.146 ± 0.118
MRT (min)	200.69 ± 3.86	276.98 ± 6.87
Brain–to–blood distribution ratio$_{(0-t)}$	0.1925 ± 0.0097	
Brain–to–blood distribution ratio$_{(0-inf)}$	0.2083 ± 0.0012	

(x ± s; n = 3)

Claudin-5, zo-1 and occludin are three of the most important tight junction proteins for maintaining BBB. Claudin-5 is an important transmembrane protein that regulates the permeability of BBB [17]. Zo-1 promotes the attachment of occludin to the cytoskeleton system, thus affecting the permeability of BBB [18]. Occludin is the first identified integral protein that localized at tight junctions [19]. High expression level of occludin is one of the important reasons for the low permeability of BBB compared to other tissue barriers. The expression level of occludin is significantly higher in cerebral vascular endothelium than in other tissues, indicating that this protein can reflect the structural and functional integrity of BBB. In this study, occludin was apparently expressed in hCMEC/D3 cells, even though its expression levels were not significantly increased over time. The expression patterns of claudin-5, zo-1 and occludin indicated that the tight junction behavior of hCMEC/D3 cells is similar to the *in vivo* environment of BBB.

In the present study, BBB permeability assays of HBA indicated that HBA could penetrate both *in vitro* and *in vivo* BBB model, and subsequently transported into the brain.

Hydrophobicity or lipophilicity of a drug affects its transport of lipid membrane, pharmacological effect, bioavailability and toxicity [20,21]. The endothelial cell membrane is lipophilic and the water–soluble compounds can hardly diffuse through the lipid membrane, thus, hydrophilic compounds are often limited by the BBB. According to Pubmed database, the lipophilicity value (XlogP3) of HBA was found to be 0.2 [22]. XlogP3 is a parameter that represents the lipophilicity of compounds, in where XlogP3 > 0 denotes that a compound distributes more in organic phase than in water. On the contrary, when XlogP < 0, the compound is more soluble in water than in organic solvent.

Tight intercellular junctions around the capillary membranes can act efficiently to slow down the drug diffusion into the brain by functioning as a thick lipid barrier. BBB limits the diffusion and penetration of hydrophilic, water–soluble and polar drugs into the brain tissue [23]. BBB permeability is one of the most important factors for determining drug absorption and bioavailability. The results of *in vitro* permeability assay indicated that HBA could pass through BBB rapidly and maintain a balance between the two sides of the *in vitro* BBB model.

Drugs diffuse along the concentration gradient, and the semi-permeable membrane can allow the diffusion of small–molecule compounds. Once the probe is in place and perfusion has started, the gradient enters the perfusate through the semi–permeable membrane. As the perfusate in the dialysis tube keeps flowing and renewing, the transmembrane concentration gradient of drug always existed and the drug can be diffused continuously. Besides, RS [24] and aCSF [25] have been reported as the main dialysis perfusates of blood and brain, respectively.

Due to the constant perfusate flow through the catheter and hence incomplete equilibrium at the membrane, only a fraction of the drug concentration can be 'recovered' in the microdialysate, which is referred as relative recovery and relative loss [26]. These parameters can be affected by several factors, such as type of drugs, drug concentration and flow rate [16]. We evaluated the relative parameters of

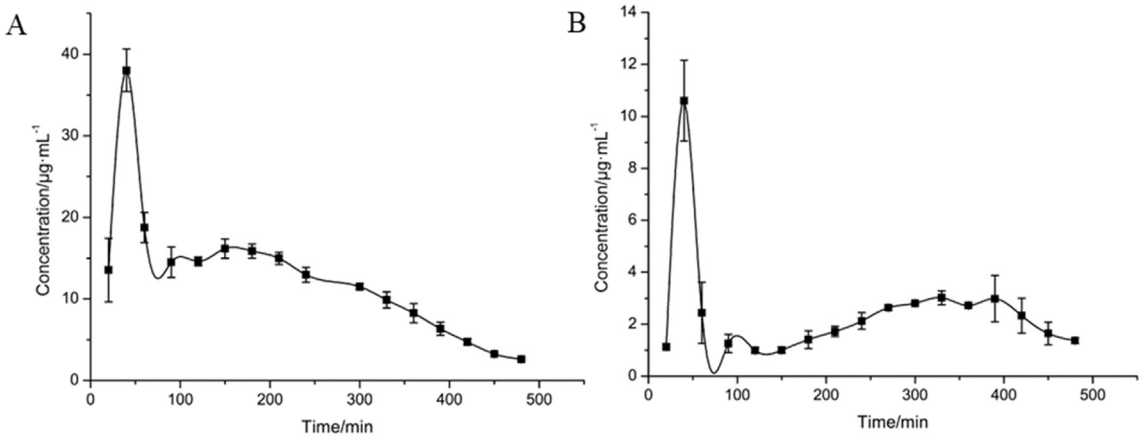

Fig. 6. Blood-brain microdialysis evaluation of HBA. (A) Time course of HBA concentration in blood. (B) Time course of HBA concentration in brain. ($x \pm s$; $n = 3$).

microdiaysis method, and the results showed that RR% and RL% could remain stable under different conditions and times. This suggests that the microdialysis method is useful and reliable for the pharmacokinetic analysis of HBA.

Next, we evaluated the pharmacokinetic parameters of HBA in the blood and brain simultaneously. The results indicated that HBA could be absorbed into the blood and brain tissue within 40 min. Approximately 20% of HBA in blood could penetrate the BBB and exert pharmacological effects on CNS disorders. However, HBA is metabolized within a short period of time, and its metabolic rate in brain tissue was much shorter than that in blood. HBA exhibited the same T_{max} in both blood and brain, but displayed shorter $t_{1/2}$ in brain than in blood. The rapid metabolism of HBA might be attributed to first–pass elimination and hepatic metabolism.

HBA is a metabolite of gastrodin (GAS), and GAS can be degraded to HBA rapidly in the blood [27]. Due to its poor permeability, the pharmacological effects of GAS may be affected by HBA biotransformation. HBA can be metabolized from GAS *in vivo*, and then passes through the BBB and preserves in the brain. Hence, the actual pharmacological activity of GAS on CNS diseases is on accounted of the remaining HBA in the brain.

The pharmacokinetic curves of HBA displayed biphasic time-concentration courses, which may be a consequence of enterohepatic circulation. After administration, HBA may undergo first-pass effect and cause decreasing concentrations in blood, followed by excretion into bile *via* hepatocytes. Afterwards, the compound enters the intestinal lumen through the biliary tract and the common bile duct. Due to its low polarity and great membrane permeability, HBA in the intestinal lumen can be absorbed by the intestinal epithelial cells and subsequently enters the blood circulation, which accounts for a double biphasic phenomenon.

In the present study, HBA penetrated hCMEC/D3 BBB model and maintained a balance between two sides. The pharmacokinetics of HBA in blood and brain after oral administration were also investigated. The brain–to–blood distribution ratio of HBA in 480 min and infinite time were 19.25% and 20.83%, respectively, suggesting that approximately 20% of HBA in blood can pass through the BBB. The brain–to–blood distribution ratio of HBA is comparable to that of some drugs against CNS disorders, including L–Dopa (treatment of Parkinson's disease, 10%) [28], meropenem (treatment of meningitis, 16%) [29] and paliperidone (anti–depression, 37%) [30]. In comparison with the poor permeability of GAS, HBA may serve as an effective compound that penetrates BBB and retains the pharmacological effects of *GE* on CNS diseases.

Author contributions

M.YK and L.MP designed the experiments. M.YH, M.YK, Ch.H, K.GH, F.CP and W.Q performed the experiments and collected the data. M.YH and M.YK analyzed and interpreted the data and was the major contributor in writing the manuscript. L.MP supervised the study. All authors read and approved the final manuscript. M.YH and M.YK contributed equally to this paper.

Funding

This study is supported by National Natural Science Foundation of China (No.81274107).

Declaration of Competing Interest

The authors declare no conflict of interest.

References

[1] L.C. Lin, Y.F. Chen, T.R. Tsai, T.H. Tsai, Analysis of brain distribution and biliary excretion of a nutrient supplement, gastrodin, in rat, Anal. Chim. Acta 590 (2007) 173–179.
[2] K. Kam, S. Yu, N. Jeong, J. Hong, A. Jalin, S. Lee, Y. Choi, C. Lee, K. Sang, P–hydroxybenzyl alcohol prevents brain injury and behavioral impairment by activating Nrf2, PDI, and neurotrophic factor genes in a rat model of brain ischemia, Mol. Cells. 31 (2011) 209–215.
[3] P. Kaengkan, S. Baek, Y. Choi, K. Kam, J. Kim, Y. Wu, B. Do, S. Kang, Combination effect of p–hydroxybenzyl alcohol and mesenchymal stem cells on the recovery of brain damage in a rat model of brain ischemia, Anim. Cells Syst. 17 (2013) 160–169.
[4] L. Gonzalez-Mariscal, A. Betanzos, P. Nava, B. Jaramillo, Tight junction proteins, Prog. Biophys. Mol. Biol. 81 (2003) 1–44.
[5] B. Weksler, I. Romero, P. Couraud, The hCMEC/D3 cell line as a model of the human blood brain barrier, Fluids and Barriers of the CNS. 10 (2013) 1–10.
[6] S. Dauchy, F. Miller, P. Couraud, R. Weaver, B. Weksler, I. Romero, J. Scherrmann, I.D. Waziers, X. Decleves, Expression and transcriptional regulation of ABC transporters and cytochromes P450 in hCMEC/D3 human cerebral microvascular endothelial cells, Biochem. Pharmacol. 77 (2009) 897–909.
[7] L. Cucullo, P. Couraud, B. Weksler, I. Romero, M. Hossain, E. Rapp, D. Janigro, Immortalized human brain endothelial cells and flow–based vascular modeling: a marriage of convenience for rational neurovascular studies, J. Cereb. Blood Flow Metab. 28 (2008) 312–328.
[8] Y.L. Lin, M.T. Wu, F.Y. Yang, Pharmacokinetics of doxorubicin in glioblastoma multiforme following ultrasound–induced blood–brain barrier disruption as determined by microdialysis, J. Pharm. Biomed. Anal. 149 (2018) 482–487.
[9] Q. Zhang, D. Wu, J. Wu, Y. Ou, C. Mu, B. Han, Q. Zhang, Improved blood–brain barrier distribution: effect of borneol on the brain pharmacokinetics of kaempferol in rats by in vivo microdialysis sampling, J. Ethnopharmacol. 162 (2015) 270–277.
[10] Y.J. Zhang, L. Wu, Q.L. Zhang, J. Li, F.X. Yin, Y. Yuan, Pharmacokinetics of phenolic compounds of Danshen extract in rat blood and brain by microdialysis sampling, J. Ethnopharmacol. 136 (2011) 129–136.
[11] Y. Jia, X. Li, H. Xie, J. Shen, J. Luo, J. Wang, K.D. Wang, Q. Liu, L. Kong, Analysis and pharmacokinetics studies of gastrodin and p–hydroxybenzyl alcohol in dogs using ultra fast liquid chromatography–tandem mass spectrometry method, J.

Pharm. Biomed. Anal. 99 (2014) 83–88.
[12] M. Hayes, L. Moen, M. Auty, T. Lea, Transport of a Prolyl Endopeptidase inhibitory peptide across the blood–brain barrier demonstrated using the hCMEC/D3 cell line Transcytosis assay, J. Agri. Food. Chem. 64 (2015) 146–150.
[13] M. Ueno, Molecular anatomy of the brain endothelial barrier:an overview of the distributional features, Curr. Med. Chem. 14 (2007) 1199–1206.
[14] N. Plock, C. Kloft, Microdialysis–theoretical background and recent implementation in applied life–sciences, Eur. J. Pharm. Sci. 25 (2005) 1–24.
[15] B. Weksler, E. Subileau, N. Perriere, P. Charneau, K. Holloway, M. Leveque, H. Tricoire-Leignel, A. Nicotra, S. Bourdoulous, P. Turowski, D. Male, F. Roux, J. Greenwood, I. Romero, P. Couraud, Blood–brain barrier–specific properties of a human adult brain endothelial cell line, FASEB J. 19 (2005) 1872–1874.
[16] H. Akiyama, T. Kondoh, T. Kokunai, T. Nagashima, N. Saito, N. Tamaki, Blood–brain barrier formation of grafted human umbilical vein endothelial cells in athymic mouse brain, Brain Res. 858 (2000) 172–176.
[17] K. Morita, H. Sasaki, M. Furuse, S. Tsukita, Endothelial claudin:claudin–5 TMVCF constitutes tight junction strands in endothelial cells, J. Cell Bio. 147 (1999) 185–194.
[18] K. Kim, Microbial translocation of the blood–brain barrier, Int. J. Parasitol. 36 (2006) 607–614.
[19] A. Ghose, T. Herbertz, R. Hudkins, B. Dorsey, J. Mallamo, Knowledge–based, central nervous system (CNS) lead selection and lead optimization for CNS drug discovery, ACS Chem. Neurosci. 3 (2011) 50–68.
[20] O. Chan, B. Stewart, Physicochemical and drug–delivery considerations for oral drug bioavailability, Drug Discov. Today 1 (1996) 461–473.
[21] R. Konsoula, F. Barile, Correlation of in vitro cytotoxicity with paracellular permeability in Caco–2 cells, Toxicol. in Vitro 19 (2005) 675–684.
[22] [dataset] NIH Pubmed Compound Summary of 4–Hydroxybenzyl Alcohol, U.S. National Library of Medicine, 2019, https://pubchem.ncbi.nlm.nih.gov/compound/125#section=Computed-Properties.
[23] L. Shargel, S. Wu, A. Yu, Applied Biopharmaceutics and Pharmacokinetics, fifth ed., McGraw–Hill, Singapore, 2005, p. 344.
[24] H. Benveniste, P.C. Huttemeier, Microdialysis–theory and application, Prog. Neurobiol. 35 (1990) 195–215.
[25] H. Huang, Y. Zhang, R. Yang, X. Tang, Determination of baicalin in rat cerebrospinal fluid and blood using microdialysis coupled with ultra–performance liquid chromatography–tandem mass spectrometry, J. Chromatogr. B 874 (2008) 77–83.
[26] D. Burau, D. Petroff, P. Simon, L. Ehmann, C. Weiser, C. Dorn, A. Kratzer, H. Wrigge, C. Kloft, Drug combinations and impact of experimental conditions on relative recovery in in vitro microdialysis investigations, Eur. J. Pharm. Sci. 127 (2018) 252–260.
[27] M. Hsieh, C. Wu, C. Chen, Gastrodin and p–hydroxybenzyl alcohol facilitate memory consolidation and retrieval, but not acquisition, on the passive avoidance task in rats, J. Ethnopharmacol. 56 (1997) 45–54.
[28] P. Huot, T.H. Johnston, J.B. Koprich, S.H. Fox, J.M. Brotchie, L–DOPA pharmacokinetics in the MPTP–lesioned macaque model of Parkinson's disease, Neuropharmacology 63 (2012) 829–836.
[29] H.L. Xin, X.R. He, W. Li, Z.D. Zhou, S. Zhang, G.J. Wang, The effect of borneol on the concentration of meropenem in rat brain and blood, J. Asian Nat. Prod. Res. 16 (2014) 648–657.
[30] S. Gustafsson, V. Lindstrom, M. Ingelsson, Hammarlund–Udenaes M and Syvanen S, intact blood–brain barrier transport of small molecular drugs in animal models of amyloid beta and alpha–synuclein pathology, Neuropharmacology 128 (2018) 482–491.